

Film Thickness Calculations in Elastohydrodynamically Lubricated Circular Contacts, Using a Multigrid Method

A. A. Lubrecht

C. H. Venner

W. E. ten Napel

R. Bosma

Twente University,
Enschede, The Netherlands

Minimum, central and average film thicknesses have been calculated for the isothermal E.H.L. point contact case, for a variety of load, rolling speed, and material parameters. The equations governing this problem were solved using a Multigrid method. This technique offers the possibility to work with a very fine grid, obtaining detailed and accurate solutions, at the cost of moderate cpu times and storage requirements, on medium size computers. Computations for low loads, requiring a large inlet zone, have been carried out using local grid refinements. The fluid in these calculations is assumed to be compressible and its viscosity-pressure behavior is described by either the Roelands equation, or the Barus equation. The ratio between the calculated minimum film thickness and the central value varied with the parameters governing the problem, but for low loads, a value of 3/4 was obtained. The film thickness behavior at these low loads can be accurately described in terms of the minimum film thickness. For higher loads, however, a description based on a film thickness, averaged over the Hertzian contact, is more appropriate to be compared with the asymptotic solution (Ertel, Grubin).

Introduction

Over the last decade, a large number of papers has been dedicated to the numerical solution of the Elasto Hydrodynamic Lubrication problem (E.H.L.). The majority of these papers dealt with the line contact case, because of its less complicated nature. Numerical techniques as Newton-Raphson and Gauss-Seidel, with underrelaxation, have been used to obtain solutions. For the point contact case, however, the solution of the problem becomes much more time-consuming, since the finite width of the contact adds another dimension to the equations. In spite of these difficulties, several successful attempts to solve the 2d problem are known from literature.

In the second half of the 70s, a breakthrough was achieved by Ranger et al. [1] and Hamrock and Dowson [2, 3]. More recently Evans and Snidle [4] obtained a solution for the heavily loaded case, using their inverse method. Chittenden et al. [5, 6], using basically the same approach as Hamrock and Dowson, calculated film thickness and pressure profiles for elliptical contacts, for different directions of lubricant entrainment.

All these solutions have been obtained using a Gauss-Seidel iterative method with underrelaxation. Since the number of Gauss-Seidel iterations, needed to obtain a converged solu-

tion, is proportional to the number of nodal points, the total work is proportional to the square of this number. Adding to this the large underrelaxation factor, it is not surprising that calculational times tend to be large for problems with order 500 points.

The large number of gridpoints, needed to obtain accurate and detailed solutions, more or less excludes the use of a Newton-Raphson method, which is commonly used nowadays for the line contact case. This is mainly so, because of the large cpu time and storage requirements. Nevertheless, Oh [7] has solved the time dependent problem using this approach, working with a relatively small number of nodal points. In contrast to these previously mentioned approaches, the Multigrid method is very well suited for the solution of numerical problems with many nodal points, as has been demonstrated by the authors for the line contact case [8] and the point contact case [9].

E. H. L. Theory

In this paper the Reynolds equation will be written in terms of the dimensionless pressure P , since the reduced pressure $q = \exp(-\bar{\alpha}P)$ cannot be applied because of the use of Roelands' pressure viscosity relation. Using the dimensionless parameters introduced in [9] (see Nomenclature), the Reynolds equation can be written as:

$$\frac{\partial}{\partial X} \left(\frac{\bar{\rho}H^3}{\bar{\eta}} \frac{\partial P}{\partial X} \right) + \frac{\partial}{\partial Y} \left(\frac{\bar{\rho}H^3}{\bar{\eta}} \frac{\partial P}{\partial Y} \right) - \lambda \frac{\partial}{\partial X} (\bar{\rho}H) = 0 \quad (1)$$

Contributed by the Tribology Division of THE AMERICAN SOCIETY OF MECHANICAL ENGINEERS and presented at the ASLE/ASME Tribology Conference, San Antonio, Texas, October 5-8, 1987. Manuscript received by the Tribology Division, February 28, 1987. Paper No. 87-Trib-47.

where

$$\lambda = \frac{12\eta_0 u R_x^2}{b^3 P_h}$$

The density is assumed to depend on the pressure according to the Dowson and Higginson relation, and the pressure viscosity relations according to Barus as well as Roelands are used.

The Barus equation reads in this notation:

$$\bar{\eta} = \exp(-\bar{\alpha}P) \quad (2)$$

while the Roelands equation can be written as:

$$\bar{\eta} = \exp\left[\frac{P_0 \bar{\alpha}}{Z} \left\{ \left(1 + \frac{P}{P_0}\right) Z - 1 \right\}\right] \quad (3)$$

where

$$P_0 = 1.96e8/P_h$$

$$Z = 0.68$$

Using second order central discretization for the first two terms of (1) and first order backward (upstream) discretization of the third term, the discretized Reynolds equation reads:

$$\begin{aligned} & \frac{\bar{\rho}_{i+1/2,j} H_{i+1/2,j}^3}{\Delta^2 \bar{\eta}_{i+1/2,j}} (P_{i+1,j} - P_{i,j}) \\ & + \frac{\bar{\rho}_{i-1/2,j} H_{i-1/2,j}^3}{\Delta^2 \bar{\eta}_{i-1/2,j}} (P_{i-1,j} - P_{i,j}) \\ & + \frac{\bar{\rho}_{i,j+1/2} H_{i,j+1/2}^3}{\Delta^2 \bar{\eta}_{i,j+1/2}} (P_{i,j+1} - P_{i,j}) \\ & + \frac{\bar{\rho}_{i,j-1/2} H_{i,j-1/2}^3}{\Delta^2 \bar{\eta}_{i,j-1/2}} (P_{i,j-1} - P_{i,j}) \\ & - \frac{\lambda}{\Delta} (\bar{\rho}_{i,j} H_{i,j} - \bar{\rho}_{i-1,j} H_{i-1,j}) = 0 \end{aligned} \quad (4)$$

The film thickness equation can be made dimensionless by the same parameters. After discretization, this equation reads:

$$H_{i,j} = H_{00} + \frac{X_i^2}{2} + \frac{Y_j^2}{2} + \frac{2}{\pi^2} \sum_k \sum_l P_{k,l}^*$$

$$\left\{ |xp| ah\left(\frac{yp}{xp}\right) + |yp| ah\left(\frac{xp}{yp}\right) + |xm| ah\left(\frac{ym}{xm}\right) \right.$$

$$\left. + |ym| ah\left(\frac{xm}{ym}\right) - |xp| ah\left(\frac{ym}{xp}\right) - |yp| ah\left(\frac{xm}{yp}\right) - |xm| ah\left(\frac{yp}{xm}\right) - |ym| ah\left(\frac{xp}{ym}\right) \right\}$$

$$\begin{aligned} \text{where } xp &= X_i - X_k + \Delta/2, \quad xm = X_i - X_k - \Delta/2 \\ yp &= Y_j - Y_l + \Delta/2, \quad ym = Y_j - Y_l - \Delta/2 \\ ah(z) &= \operatorname{arcsinh}(z) = \ln(z + \sqrt{1+z^2}) \\ \Delta &= X_i - X_{i-1} = Y_j - Y_{j-1} \end{aligned} \quad (5)$$

The third equation, describing the force balance, gives:

$$\sum_i \sum_j \Delta^2 P_{i,j} - \frac{2\pi}{3} = 0 \quad (6)$$

Multigrid Method

A short description of the Multigrid technique, applied to the E.H.L. point contact problem, is given in [9]. For a more general and detailed treatment of this matter the reader is referred to Brandt [10, 11] and Hackbusch [12].

Local Grid Refinements

When using Multigrid techniques, there is no reason why a finer grid should extend over the same region as the coarser ones. This gives the user the opportunity to place increasingly finer grids over increasingly smaller subdomains. The idea is to use finer grids only locally, for instance in regions where large gradients in the solution occur, see Fig. 1. The only restriction is, that a finer grid may not extend beyond its next coarser grid. For more information the reader is referred to Brandt [11] and Venner [14].

For the E.H.L. point contact problem, this means that the finest grid will only be used in the Hertzian region, while increasingly coarser grids are used to cover the inlet zone. This large inlet zone is needed in the low loaded case, to avoid "numerically" starved lubrication.

When all grids extend over the same domain it is almost impossible to obtain accurate solutions for these low load conditions because the requirement of using a fine grid results in excessive computational costs.

Analytical Solutions

Where the three asymptotic solutions for the line-contact

Nomenclature

b = the contact radius		
E' = reduced Youngs modulus, $2/E' = (1 - \nu_1^2)/E_1 + (1 - \nu_2^2)/E_2$	parameter according to Moes, $L = G(2U)^{1/4}$	Y = dimensionless coordinate, $Y = y/b$
G = dimensionless material parameter according to Hamrock and Dowson $G = \alpha E'$	M = dimensionless load parameter according to Moes, $M = W(2U)^{-3/4}$	α = pressure viscosity coefficient according to Barus
H = dimensionless film thickness, $H = hR_x/b^2$	P = dimensionless pressure, $P = p/P_h$	$\bar{\alpha}$ = dimensionless pressure viscosity coefficient, $\bar{\alpha} = \alpha P_h$
H_{hd} = dimensionless film thickness according to Hamrock and Dowson $H_{hd} = h/R_x$	P_h = maximum Hertzian pressure	Δ = distance between two neighboring gridpoints
H_{00} = dimensionless constant	R_x = reduced radius of curvature	η = viscosity
H' = dimensionless minimum film thickness according to Moes, $H' = H_{hd}(2U)^{-1/2}$	u = tangential velocity (mean velocity) $u = (u_1 + u_2)/2$	η_0 = viscosity at atmospheric conditions
H'_c = dimensionless central film thickness (at $dP/dX = 0$)	U = dimensionless velocity according to Hamrock and Dowson $U = \eta_0 u/E'R_x$	$\bar{\eta}$ = dimensionless viscosity, $\bar{\eta} = \eta/\eta_0$
H' = dimensionless average film thickness	u_Σ = sum velocity $u_\Sigma = u_1 + u_2$	ρ = density
L = dimensionless material	w = load	ρ_0 = density at atmospheric conditions
	W = dimensionless load according to Hamrock and Dowson, $W = w/E'R_x$	$\bar{\rho}$ = dimensionless density, $\bar{\rho} = \rho/\rho_0$
	X = dimensionless coordinate, $X = x/b$	λ = dimensionless velocity parameter

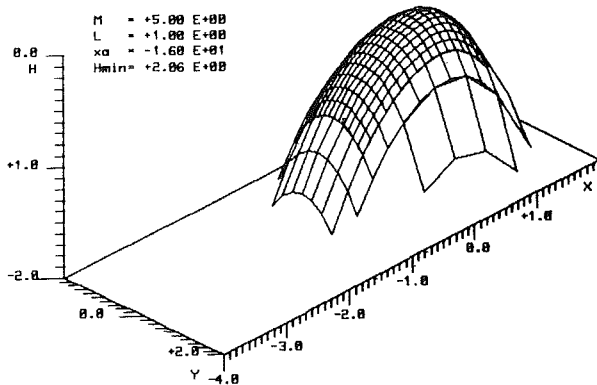
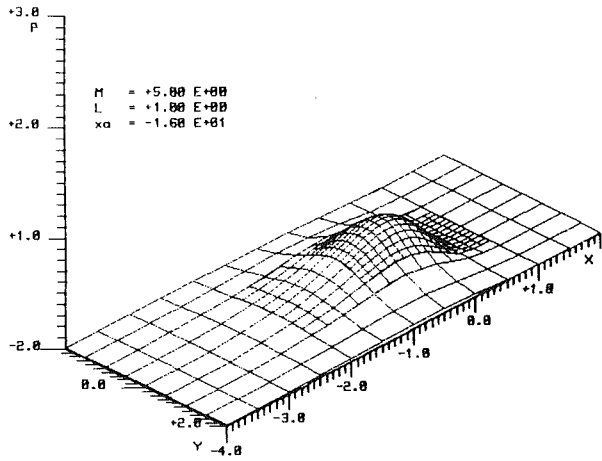


Fig. 1 Pressure and film thickness distribution using local grid refinements, $M=5$, $L=1$, $X_a = -16$, $Y_a = -8$

case can be combined to serve as a solution for the full problem (see [13]) just one asymptote is known from literature, for the point-contact problem. The rigid-iso-viscous asymptote was calculated by Brewster et al. [15] as:

$$H' = 34/M^2 \quad (7)$$

More accurate calculations by Venner [14], using Multigrid techniques, show that the constant is 35.5.

Venner also calculated the Grubin type asymptote i.e.,

$$\bar{H}' = 1.02 L^{3/4} M^{-1/12} \quad (8)$$

assuming the pressure distribution to be rotational symmetric and the film thickness to be parallel. These asymptotes can be compared with the full numerical solution, see Figs. 2 and 4. No two-dimensional equivalent of Herrebrugh's solution is known to the authors.

Calculational Details

As was found for the line-contact case [13], the use of the second order backward discretization of the third term in equation (1), resulted in more accurate values for the minimum film thickness, using relatively few points. However, this second order accurate discretization gave no converging solutions for high loads.

Most solutions presented in this paper, have been calculated using the first order backward discretization of the third term in equation (1), see equation (4), using almost 3000 points, consuming two hours of cpu time on a VAX11/750. For the calculations using local grid refinements, the computing time was half an hour.

For the high load conditions, all grids extended over the

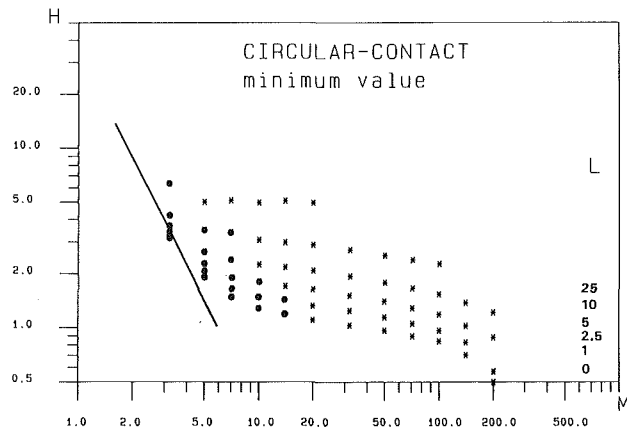


Fig. 2 Minimum film thickness graph, the full circles represent the solutions obtained with a larger domain. The drawn line is the isoviscous-rigid asymptote, equation (7)

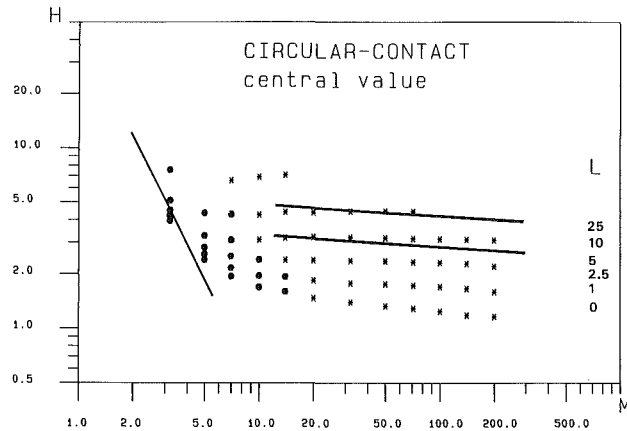


Fig. 3 Central film thickness graph, the full circles represent the solutions obtained with a larger domain. The drawn lines are the film thickness values predicted by Chittenden et al., equation (10) ($L=5$, $L=10$) and the isoviscous-rigid asymptote, equation (7).

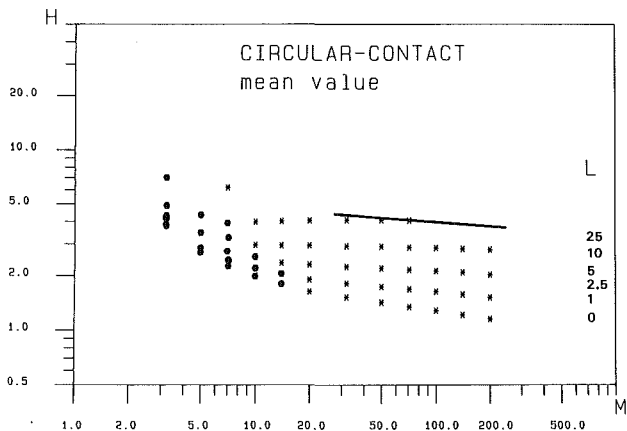


Fig. 4 Average film thickness graph, the full circles represent the solutions obtained with a larger domain. The drawn line is the film thickness according to the Grubin asymptote, equation (8), $L=10$.

same domain, the inlet was at $X = -4$, while the width of the domain was twice the Hertzian radius. For the low loaded case, local grid refinement techniques were used, the coarsest grid started at $X = -16$ and $Y = -8$, while generally the finer grids covered only a quarter of the domain of the next coarser level. Convergence of the solution up to truncation errors of the discretized equations, was checked as described in [9] and by Brandt [11].

Table 1 Ratio H_c/H_m as a function of L and M

$M =$	7	10	14	20	32	50	71	100	141	200
$L =$										
0	1.3	1.3	1.3	1.3	1.4	1.4	1.5	1.6	2.0	3.2
1	1.3	1.3	1.3	1.4	1.4	1.5	1.6	1.8	2.1	2.7
2.5	1.3	1.3	1.4	1.5	1.6	1.6	1.8	2.0	2.2	2.5
5	1.3	1.4	1.4	1.5	1.6	1.8	1.9	2.0	2.2	2.4
10	1.3	1.4	1.4	1.5	1.6	1.7	1.8	—	—	—
25	1.2	1.3	1.3	—	—	—	—	—	—	—

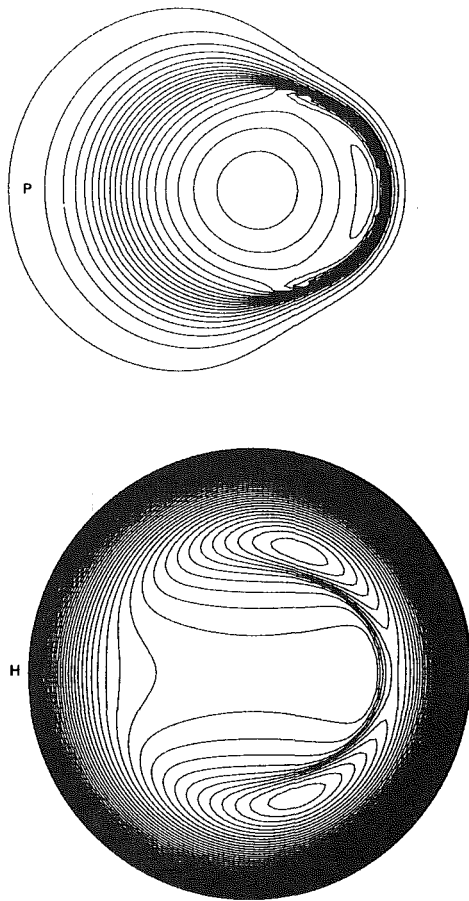


Fig. 5 Pressure- (P) and film thickness (H) contour plot, using 11505 points for $M=32$, $L=10$, $\Delta P=0.05$, $\Delta H=0.01$. The dark region of large gradients in the film thickness coincides with the pressure spike region.

Results

Contrary to the line contact case, the point contact case does not give a constant ratio between the central and the minimum film thickness.

For the low loads, the ratio of H_c/H_m was 4/3. For higher loads however, large deviations occurred, as was reported by Chittenden et al. In Table 1 the value of H_c/H_m is given as a function of the dimensionless parameters L and M .

In Fig. 1 a plot is presented of the pressure distribution and the film thickness profile for a low loaded case, using the local grid refinement technique. For the low load case, the minimum film thickness was found along the central line of the contact, while for higher loads, it was located in the side lobes. Because of the nonconstant ratio of H_c/H_m , it was not possible to present the results of these calculations in one formula, as was done for the line contact case [13]. For low M -values, the minimum film thickness can be described by a Martin-Gümbel type of analysis, (equation (7), Fig. 2). For high M values, a Grubin type of analysis is needed, assuming a constant film thickness throughout the Hertzian contact zone.

To be able to compare the numerical results with this asymptotic solution, an average film thickness \bar{H} is introduced, defined as:

$$\bar{H} = \frac{1}{\Omega} \int_{\Omega} H(X, Y) dX dY \tag{9}$$

integrating over the Hertzian zone Ω

From Figs. 2 and 3 it can be seen that the minimum film thickness for low M values tends to be too low due to the “numerical” starvation effect. For the low M values ($M < 10$) an even larger inlet zone should be used, resulting in the need to use an infinite domain for the asymptotic isoviscous-rigid case. From Fig. 2, an additional decrease of the film thickness can be detected for high M values, due to the small film thickness values in the side lobes, see also Table 1. For small values of M the minimum film thickness is found along the X -axis of the contact while for higher values of M it moves to the side lobes. Contrary to Fig. 2, the central film thickness in Fig. 3, shows no signs of an additional decrease for high M values.

In Fig. 3 the numerical results are compared with the formula derived by Chittenden et al. for the central film thickness:

$$H'_c = 1.75 L^{0.49} M^{-0.073} \tag{10}$$

It can be seen that the results are in reasonable agreement. The numerically calculated values are somewhat larger than the values predicted by this formula. Also it can be concluded that the dependency of the central film thickness is somewhat smaller than predicted by Chittenden’s formula. All results have been calculated for a compressible fluid, using Roelands’ pressure viscosity relation.

Similar to the line-contact problem [13] the differences in the solution when using the Barus pressure viscosity equation instead of Roelands’ were small. The results of the calculations using the extended inlet are given in full circles.

Taking advantage of the possibility to use many calculational points, the effect of the pressure spike on the film thickness profile can be studied. As can be seen from the Reynolds equation (1), regions where the second derivative of the pressure is large (the pressure spike) should coincide with a region where the first derivative of the film thickness is large. Figure 5 shows a pressure- and a film thickness contour plot for the case $M=32$, $L=10$, which is heavily spiked, using almost 12,000 points. In the film thickness plot a horseshoe-shaped region can be detected where the film thickness gradients are large and this is indeed the pressure spike region. This knowledge can perhaps be used to study the pressure spike from optical interference measurements of the film thickness profile.

Conclusions

Film thickness distributions have been calculated for a variety of conditions and local grid refinements were used to cover a large inlet region at low loads. The calculated low load minimum film thickness values agrees quite well with the isoviscous-rigid asymptote (Fig. 2), though for very low values of M , a larger inlet zone is needed. For $L=10$, $M > 20$ the average film thickness is accurately predicted by the Grubin

asymptote (equation (8), Fig. 4), although the numerically calculated slope is less than the predicted one. This can be explained with the results of Table 1; the side lobes form an increasingly effective seal against side leakage. Grubin's analysis does not account for this effect. For lower values of L , the influence of the isoviscous-elastic asymptote becomes increasingly important, and the Grubin asymptote predicts a too low value for the actual film thickness.

The ratio between the central and the minimum film thickness is found to be $4/3$ for low loads, but increases fast for higher loads. For these high loads, the minimum film thickness is located in the side lobes.

To obtain one single formula that predicts the film thickness throughout the entire range of conditions, the central film thickness is best suited, since the Grubin asymptote can also be used, but unfortunately, it is less interesting for practical purposes. However, to accomplish this, an expression for the elastic-isoviscous asymptote has to be found first.

Acknowledgment

The authors would like to thank Prof. Dr. A Brandt of the Weizmann Institute of Science for the many discussions and suggestions on the Multigrid approach. Part of this work was done during a stay at the Weizmann Institute of Science, Israel, supported by the "Stichting ter Bevordering van de Tribologie" and a grant from AFOSR 86-0127.

References

- 1 Ranger, A. P., Ettles, C. M., and Cameron, A., "The Solution of the Point Contact Elastohydrodynamic Problem," *Proc. R. Soc. London, Series A* 346, 1975, pp. 227-244.
- 2 Hamrock, B. J., and Dowson, D., "Isothermal Elastohydrodynamic Lubrication of Point Contacts, Part I: Theoretical Formulation," *ASME JOURNAL OF LUBRICATION TECHNOLOGY*, Vol. 98, 1976, pp. 223-229.
- 3 Hamrock, B. J., and Dowson, D., "Isothermal Elastohydrodynamic

Lubrication of Point Contacts, Part III: Fully Flooded Results," *ASME JOURNAL OF LUBRICATION TECHNOLOGY*, Vol. 99, 1977, pp. 264-276.

- 4 Evans, H. P., and Snidle, R. W., "The Elastohydrodynamic Lubrication of Point Contacts of Heavy Loads," *Proc. R. Soc., London, Series A* 382, 1982, pp. 183-199.

- 5 Chittenden, R. J., Dowson, D., Dunn, J. F., and Taylor, C. M., "A Theoretical Analysis of the Isothermal Elastohydrodynamic Lubrication of Concentrated Contacts. I: Direction of Lubrication Entrainment Coincident With the Major Axis of the Hertzian Contact Ellipse," *Proc. R. Soc., London, Series A* 397, 1985, pp. 245-269.

- 6 Chittenden, R. J., Dowson, D., Dunn, J. F., and Taylor, C. M., "A Theoretical Analysis of the Isothermal Elastohydrodynamic Lubrication of Concentrated Contacts. II: General Case, With Lubricant Entrainment Along Either Principle Axis of the Hertzian Contact Ellipse or at Some Intermediate Angle," *Proc. R. Soc., London, Series A* 397, 1985, pp. 271-294.

- 7 Oh, K. P., "The Numerical Solution of Dynamically Loaded Elastohydrodynamic Contact as a Nonlinear Complementary Problem," *ASME JOURNAL OF TRIBOLOGY*, Vol. 106, 1985, pp. 88-95.

- 8 Lubrecht, A. A., ten Napel, W. E., and Bosma, R., "Multigrid, an Alternative Method for Calculating Film Thickness and Pressure Profiles in Elastohydrodynamically Lubricated Line Contacts," *ASME JOURNAL OF TRIBOLOGY*, Vol. 108, 1986, pp. 551-556.

- 9 Lubrecht, A. A., ten Napel, W. E., and Bosma, R., "Multigrid, an Alternative Method of Solution for Two-Dimensional Elastohydrodynamically Lubricated Point Contact Calculations," presented at the ASME/ASLE Joint Conference, October 1986, to be published in the *ASME JOURNAL OF TRIBOLOGY*.

- 10 Brandt, A., "Multi-Level Adaptive Solutions to Boundary-Value Problems," *Math. of Comp.*, Vol. 31, 138, 1977, pp. 333-390.

- 11 Brandt, A., "Multigrid Techniques: 1984 Guide With Applications to Fluid Dynamics," Monograph. Available as G.M.D.-studie No. 85 from G.M.D.-FIT, postfach 1240, D-5205, St. Augustin 1 W. Germany.

- 12 Hackbusch, W., *Multi-Grid Methods and Applications*, Springer Verlag, 1985.

- 13 Lubrecht, A. A., Breukink, G. A. C., Moes, H., ten Napel, W. E., and Bosma, R., "Solving Reynolds' Equation for e.h.l. Line Contacts by Application of a Multigrid Method," presented at the Leeds/Lyon Conference, Sept. 1986.

- 14 Venner, C. H., Ma. Sc. thesis, Twente University, 1987, The Netherlands (in Dutch).

- 15 Brewse, D. E., Hamrock, B. J., and Taylor, C. M., "Effect of Geometry on Hydrodynamic Film Thickness," *ASME JOURNAL OF TRIBOLOGY*, Vol. 101, 1979, pp. 231-239.